Environmental Sciences Europe

RESEARCH

Open Access

Comparative study on the novel bare and immobilized forms of phyco-synthesized Ag-Fe bimetallic nanoparticles for bioremediation of aquaculture wastewater

Ahlam S. El Shehawy[1*], Elham M. Ali[2,3*] and Ashraf Elsayed[1]

Abstract

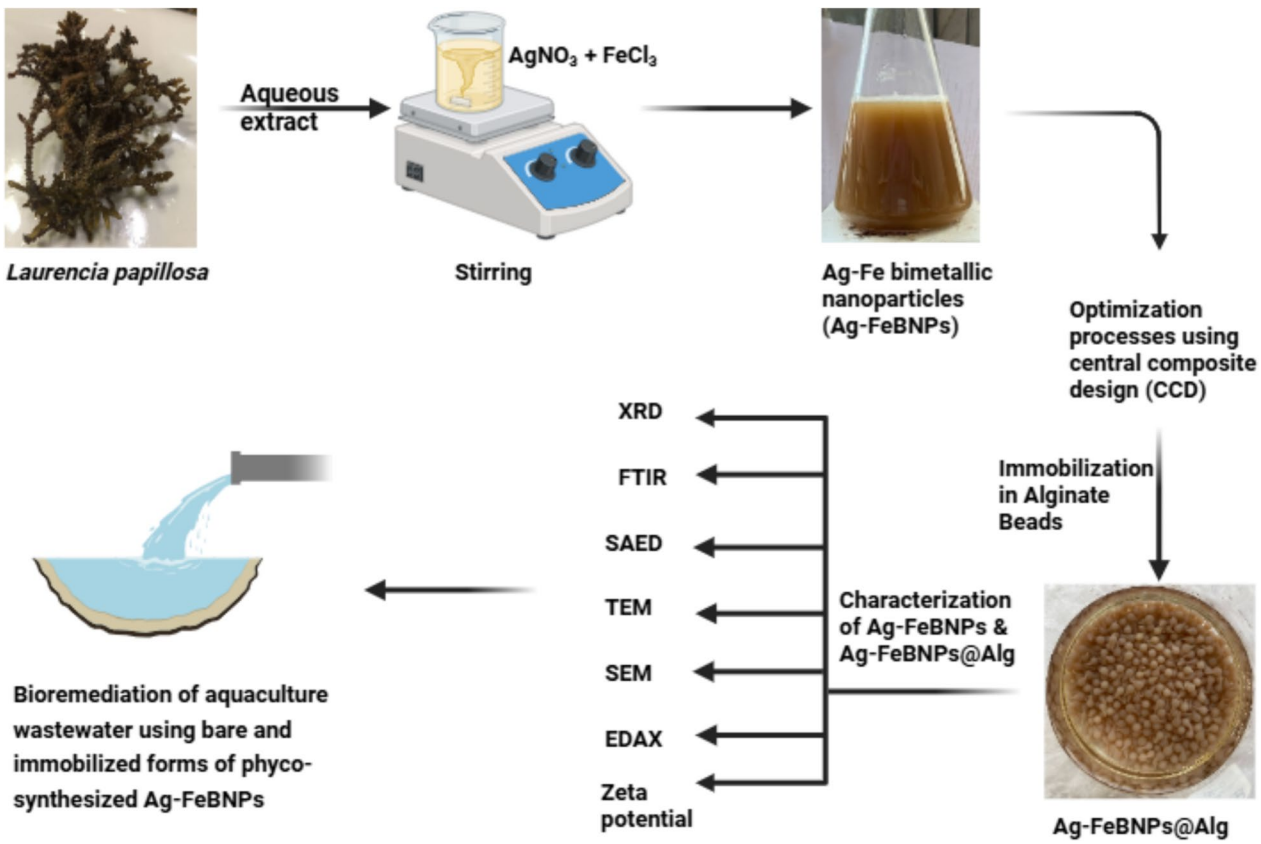
Green synthesized Ag-Fe bimetallic nanoparticles (Ag-FeBNPs) offer a promising candidate for heavy metal removal thanks to their exceptional properties, efficiency in adsorption processes, stability, enhanced catalytic activity, and eco-friendliness. The current work uses the red alga; *Laurencia Papillosa* for a novel synthesis of the Ag-FeBNPs, which has been prepared in two different forms; bare and immobilized to test the efficiency of the Ag-FeBNPs at the first stage and to compare the potentiality of both forms for the bioremediation process. This study introduces a novel bio-inspired synthesis route using *L. Papillosa*, which has not been previously reported for Ag-FeBNPs, highlighting the distinctive phycochemical reduction mechanism as a key element of novelty. The optimal parameters for this bimetallic synthesis were established via the central composite design (CCD), which set the pH at 10 and employed 10.5 g of algae/100 mL water for 95 min. The alginate beads were used to immobilize the optimized Ag-FeBNPs (Ag-FeBNPs@Alg beads) as a strategy to mitigate the potential toxicity of bare nanoparticles. Bare and immobilized phyco-synthesized Ag-FeBNPs were investigated for Fe and Zn removal from aquaculture wastewater. Results indicated significant removal ratios for Fe and Zn with 94.8% and 76.0% when using the bare Ag-FeBNPs and 78.0% and 45.5% when using Ag-FeBNPs@Alg beads, respectively. Qualitative observations further revealed improved particle dispersion, high adsorption affinity, and enhanced surface functional group interactions in the bare form, whereas the immobilized form showed greater operational handling, safety, and reusability. Various characterization approaches, including Scanning Electron Microscope (SEM) and Fourier transform infrared (FTIR) spectroscopy, were employed to confirm the synthesis of Ag-FeBNPs forms and their role in metal removal. The results proved that Ag-FeBNPs@Alg beads are simply prepared, practically utilized, and relatively low in cost. These characteristics reveal their potential as a promising adsorbent for heavy metals removal from wastewater not only at small or bench-scale but also with potential for large-scale and commercial applications in aquaculture and industrial wastewater treatment systems.

Keywords Phyco-synthesis, *Laurencia papillosa*, Ag-Fe bimetallic nanoparticles, Immobilized nanoparticles, Alginate beads, Heavy metal removal

*Correspondence:
Ahlam S. El Shehawy
ahlam.saleh@outlook.com
Elham M. Ali
elhamali@narss.sci.eg
Full list of author information is available at the end of the article

© The Author(s) 2026. **Open Access** This article is licensed under a Creative Commons Attribution 4.0 International License, which permits use, sharing, adaptation, distribution and reproduction in any medium or format, as long as you give appropriate credit to the original author(s) and the source, provide a link to the Creative Commons licence, and indicate if changes were made. The images or other third party material in this article are included in the article's Creative Commons licence, unless indicated otherwise in a credit line to the material. If material is not included in the article's Creative Commons licence and your intended use is not permitted by statutory regulation or exceeds the permitted use, you will need to obtain permission directly from the copyright holder. To view a copy of this licence, visit http://creativecommons.org/licenses/by/4.0/.

Graphical abstract



Introduction

Most hydrological resources are under pressure at the global level either due to drought or pollution [1, 2]. Heavy metal pollution seriously threatens water quality, ecological balance, and human well-being [3–5]. Recently, increasing attention has been directed toward the application of algae-based systems for the remediation of potentially toxic elements from agricultural and industrial wastewater [6]. Phycoremediation, in particular, has shown great promise as a cost-effective and eco-friendly strategy, as algae can act both as biosorbents and as biofactories for nanoparticle synthesis [7]. Several studies proved that the unique characteristics of nanoparticles at the nanoscale, including enhanced catalysis and adsorption, make them highly effective in wastewater treatment [8–10]. Furthermore, nanomaterials have been extensively utilized in a wide range of other applications, including antimicrobial coatings, catalysis, biosensing, and environmental cleanup technologies, which underscores their broad scientific and industrial relevance [11, 12]. Biologically-based synthesis of NPs [13–16], particularly those algae-based ones [17, 18], is successfully used for water remediation due to their potential cost-effectiveness, nontoxicity, large-scale production, and minimal environmental impact. Silver nanoparticles (AgNPs) are among the most extensively studied nanomaterials due to their strong antimicrobial activity, high surface reactivity, and catalytic potential. In environmental applications [19]. Their nanoscale size and large surface area provide enhanced adsorption and interaction with pollutants, while their stability supports repeated use in treatment processes [20, 21]. However, concerns regarding their potential cytotoxicity and the uncontrolled release of silver ions into the environment may restrict their large-scale applications in bioremediation [22]. Iron nanoparticles (FeNPs) have a strong reducing capacity and are considered environmentally friendly, cost-effective, and highly efficient in site-specific remediation [12, 16]. Nonetheless, their tendency to aggregate and undergo surface oxidation can reduce their reactivity and long-term stability, which limits their efficiency when used alone [23].

Ag-FeBNPs, unlike their monometallic and bulk counterparts, provide a significant advantage in heavy metal removal with high adsorption efficiency, stability, and enhanced catalytic activity together with eco-friendliness [24, 25]. In addition, their bimetallic composition improves redox potential, accelerates electron transfer, and enhances the degradation of a wide range of organic and inorganic pollutants [26]. Such unique properties make Ag-FeBNPs highly effective for wastewater treatment and represent a sustainable and versatile nanomaterial for bioremediation applications.

One of the disadvantages of using Ag-FeBNPs in water purification is the potential metal release during the treatment process, causing adverse consequences for both ecosystems and human health [27]. A new strategy for utilizing nanoparticles as adsorbents was implemented to hinder or minimize this effect through the encapsulation of alginate beads [28]. This method traps the NPs, prevents the metal release in the medium, and allows for efficient reuse with potential recovery of the adsorbed material [29, 30].

In this research, we explore a novel eco-friendly approach for using *Laurencia papillosa* alga as a mediator for the phycho-synthesis of Ag-FeBNPs. To our knowledge, this work pioneered the green synthesis of Ag-FeBNPs from *Laurencia papillosa*. A patent for this innovation has been submitted nationally to the Egyptian Patent Office with the number EG/P/2024/330. The phycho-synthesized Ag-FeBNPs were also optimized and encapsulated in alginate beads (Ag-FeBNPs@Alg). The central objective of this study is to evaluate and compare the performance of both bare and immobilized Ag-FeBNPs for the removal of Fe and Zn from aquaculture wastewater, thereby assessing their effectiveness and potential for practical bioremediation applications. This study is significant as it introduces a previously unreported red alga-based route for bimetallic Ag-FeBNPs synthesis, providing new insights into phycochemical reduction mechanisms. The combined optimization and immobilization strategy presented here demonstrates a novel, safer, and more practical approach for nanoparticle use in real wastewater systems. In addition, compared with previous studies that used non-immobilized or monometallic nanoparticles, the Ag-FeBNPs@alg system offers clear advantages in terms of safer handling, lower metal leaching, improved long-term stability, and greater practicality for real wastewater applications. This work further offers a potentially scalable and commercially relevant platform for sustainable heavy-metal removal, particularly within aquaculture and industrial treatment operations.

Materials and methods

Materials

All required solutions (e.g., silver nitrate, ferric chloride, sodium alginate, and calcium chloride) were prepared using deionized water. The marine red alga *Laurencia papillosa* was collected from Al-Zaafarana beach (29.06° N, 32.43° E), a location at the Suez Gulf, The Red Sea, Egypt.

Ag-FeBNPs phyco-synthesis and optimization processes

Fresh seaweed samples were washed thoroughly with seawater, tap water, and distilled water to remove epiphytes and debris. The cleaned samples were air-dried in shade for two weeks, ground into fine powder using liquid nitrogen, and stored in air-tight containers at 4 °C until further use [31]. About 5g of crushed dried algal powder was used to prepare the extract of which the supernatants were used to prepare the Ag-FeBNPs [32]. Phyco-synthesis of Ag-FeBNPs was achieved by mixing $AgNO_3$ (20 mL, 0.01 M) and $FeCl_3$ (20 mL, 0.01 M) under continuous stirring for about 20 min while adding about 20 mL of fresh extract to the Ag-Fe solution with constant stirring. The reaction progress was monitored by visual observation [33]. A central composite design (CCD) was employed to investigate the individual and interactive influences of pH, the concentration of algae extract (g/100 ml), and time (min) on the surface plasmon resonance (SPR) absorbance [34, 35]. A 20-run design of the experiment was executed using the Design Expert Version 8.0 software (Stat-Ease, Inc., Minneapolis, MN, USA). A second-order polynomial model was fitted to the experimental data, including five replicates at the center point (Table 1).

Immobilization of the optimized Ag-FeBNPs in alginate beads

Ag-FeBNPs were immobilized in alginate beads (Ag-FeBNPs@Alg) following the method described by Bezbaruah et al. [36]. Alginate (3% w/v) and Ag-FeBNPs solutions were combined in a 1:1 ratio and mixed for 0.5 h to form a homogeneous gel. Spherical beads were formed by

Table 1 Variable levels were used in the CCD experiment on Ag-FeBNPs

Variables	Levels				
	−2	−1	0	+1	+2
pH	3.0	4.9	7.0	9.4	11.0
The concentration of algal extract (g/100 mL)	1.0	4.9	10.5	16.1	20
Time (min)	10	44	95	146	180

droplet addition into a 0.05 M $CaCl_2$ solution with constant stirring and allowed to harden for 24 h.

Experimental design for heavy metal removal

The primary objective of this study was to compare the efficiency of both bare and immobilized phyco-synthesized Ag-FeBNPs forms for water treatment and heavy metal removal, particularly iron (Fe), and zinc (Zn). Wastewater was collected from a running fish aquaculture farm in Port Said Governorate, Egypt, of which 100 ml were filtered and mixed with 0.2 g/L bare Ag-FeBNPs at a constant speed (120 rpm) and room temperature (25 °C) for 95 min. The specimen was centrifuged at high speed (4000 rpm) for 15 min to separate the NPs. A parallel experiment was conducted using Ag-FeBNPs@Alg beads at the same dosage (0.2 g) to compare the effect of immobilization in alginate.

The analytical determination of Fe and Zn in the water before and after treatment was performed using the inductively coupled plasma technique (ICAMS). The percentages of Fe and Zn were calculated using Eq. 1.

$$\%R = \frac{C_0 - C_t}{C_0} \times 100 \quad (1)$$

where C_o is the concentration of Fe, Zn, and Mn before treatment (mg/L), while C_t is the concentration of Fe and Zn after treatment (mg/L).

Characterization of Ag-FeBNPs and Ag-FeBNPs@Alg

Concerning bar Ag-FeBNPs, the crystal lattice, phase purity, and particle size were determined using XRD (DX-1000 X-ray powder diffractometer) [37]. The main components of *Laurencia papillosa* extract and the biomolecules involved in the phyco-synthesis of Ag-FeBNPs were analyzed using FTIR (Burker Vertex 80) in the 400–4000 cm^{-1} range [38]. The average size, infrastructure, and Selected Area Electron Diffraction [12] patterns of Ag-FeBNPs were visualized using TEM (JEOLJEM-2100) [39]. The size, shape, and morphologies of Ag-FeBNPs were examined using SEM (JEOL JSM-6510LV). The elemental composition of Ag-FeBNPs was analyzed using EDAX attached to the SEM. [40]. Nano-colloidal solution stability and surface charge of Ag-FeBNPs were measured using Photon Correlation Spectroscopy (Malvern Zeta size Nano-zs90, U.S.A) [41].

Concerning Ag-FeBNPs@Alg beads, Morphological features, physical organization, and elemental composition of Ag-FeBNPs@Alg beads were analyzed using SEM and EDAX before and after treatment of fish aquaculture wastewater effluents. FTIR spectra of Ag-FeBNPs@Alg beads were recorded before and after treatment to assess changes in biomolecular composition.

Evaluation of the reuse potentiality of Ag-FeBNPs@Alg beads

The beads loaded with heavy metals were subjected to 0.1 N HCl for 60 min for metal ions recovery, followed by washing with double-distilled water [42]. The regenerated beads were then again reused in fish aquaculture wastewater effluents for the next adsorption run. Four runs of adsorption–desorption experiments were conducted to evaluate the reuse potentiality of Ag-FeBNPs@Alg beads to retain heavy metal removal.

Results

Characteristics of bare phyco-synthesized Ag-FeBNPs

Before the phyco-synthesis of Ag-FeBNPs, the collected alga was morphologically characterized and identified as *Laurencia obtusa* var. *papillosa* (C.Agardh), a red alga belonging to the Rhodophyta phylum (Fig. 1a) [43, 44]. Adding *L. papillosa* extract to the Ag-Fe solution resulted in a colour change to dark brown, indicating the potential formation of Ag-FeBNPs (Fig. 1b, c).

X-ray diffraction pattern of Ag-FeBNPs exhibited characteristic peaks at 28.25^0, 29.34^0, 31.57^0, 40.49^0, 46.31^0, and 50.31^0 corresponding to the (210), (220), (104), (114), (231), and (042). XRD analysis reveals the characteristic diffraction peaks of Ag (JCPDS no. 04-0783) and Fe (JCPDS no. 33-0664), indicating the successful synthesis of a bimetallic structure (Fig. 2a). FTIR analysis of phyco-synthesized Ag-FeBNPs and *L. papillosa* extract revealed similar spectral patterns, with key peaks at 3421, 1598, 1384, 1035, and 865 $cm^{-1}$are associated with N–H, O–H, C=C, N–O, and O–H stretching and bending, respectively suggesting the presence of amine, alcohol, alkene, nitro, and carboxylic acid functional groups (Fig. 2b).

The TEM micrographs displayed a nano range spherical shaped morphology with no aggregation or agglomeration with particles that ranged from 10.17 to 19.99 nm (Fig. 3a, b, c). The SAED pattern reveals the polycrystalline nature of Ag-FeBNPs, characterized by distinct dot and ring patterns (Fig. 3d).

The characteristic peaks observed in the EDAX spectrum at 3 keV, 6 keV, 6.6 keV, and 0.5 keV corroborated the phyco-synthesis of Ag-FeBNPs (Fig. 4) that composed of Fe contains 12.85% as to weight percentage 5.36 as an atomic percentage and Ag contains 37.77% as to weight percentage 8.16% as an atomic percentage. The inset SEM micrograph in Fig. 4 showed that some nanoparticles agglomerated together to form larger irregular clusters with uniform surfaces. The phyco-synthesized Ag-FeBNPs exhibited a negative zeta potential of -17.2 mV, as shown in Fig. 5.

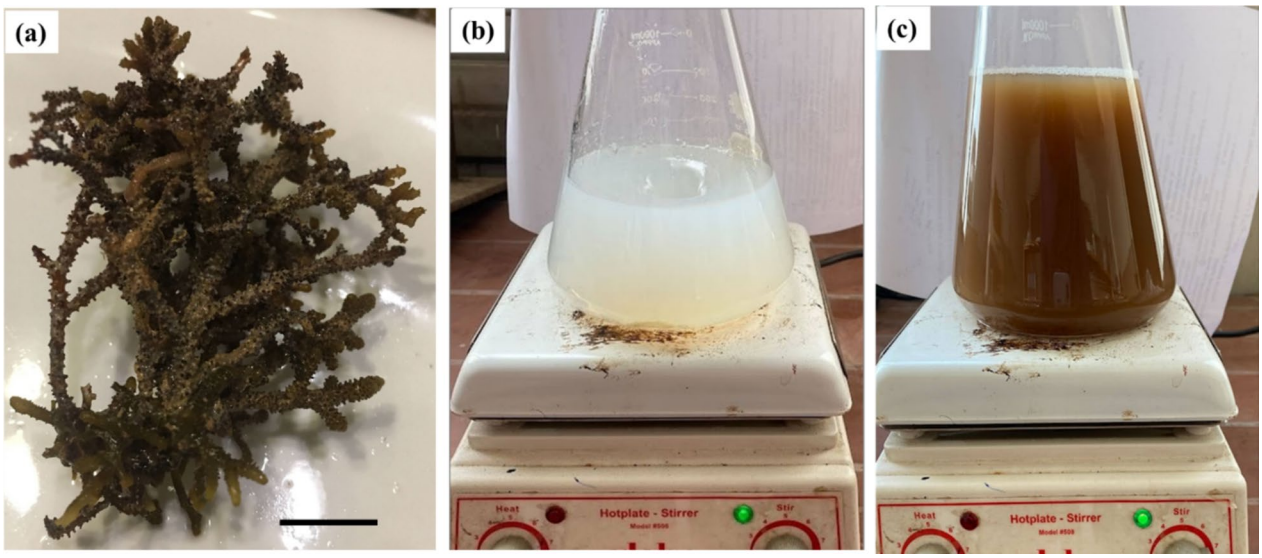


Fig. 1 Photographs representing **a** the picked red alga *Laurencia papillosa* (scale bar = 2 cm), and the visual observation of colour change in the reaction mixture from **b** the initial Ag-Fe solution to **c** a dark brown colour after the addition of the aqueous extract of *Laurencia papillosa*, indicating the formation of Ag-Fe bimetallic nanoparticles

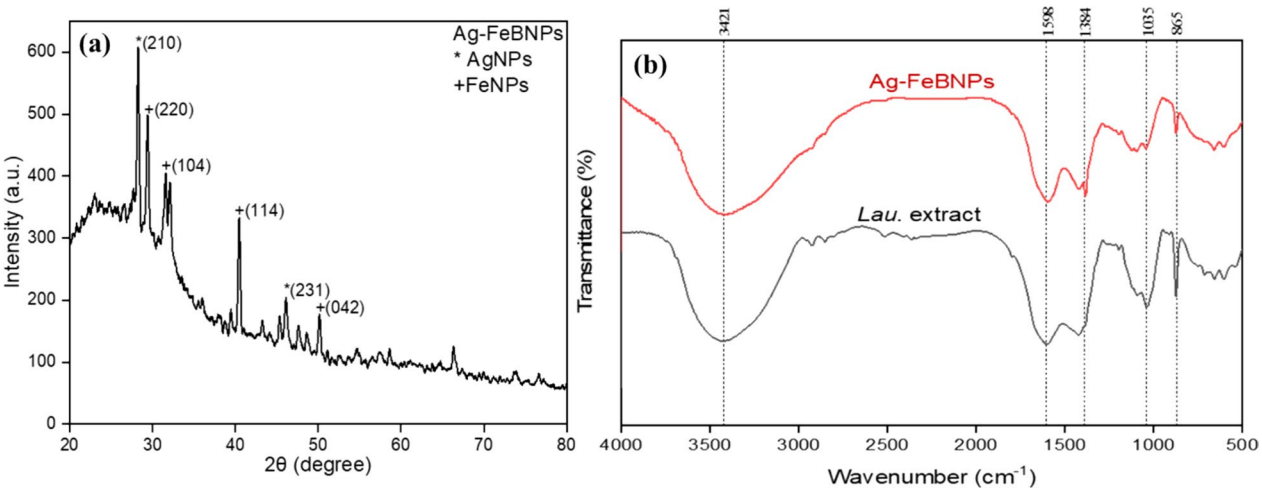


Fig. 2 **a** XRD patterns of phyco-synthesized Ag-FeBNPs and **b** FTIR spectrum of *Laurencia papillosa* extract and Ag-FeBNPs

Optimizing conditions for phyco-synthesis of Ag-FeBNPs

Table 2 summarizes the results of 20 experiments designed to optimize the phyco-synthesis of Ag-FeBNPs from *Laurencia papillosa* using CCD. Run No 16, with a pH of 10, an algae concentration of 10.5 g/100 mL, and a reaction time of 95 min, was identified as the optimal condition for phyco-synthesis. Under these conditions, the maximum absorbance at 263 nm was 11. The 3D response surface plots (Fig. 6) illustrate how pH, concentration, and time influence the SPR intensity of Ag-FeBNPs. Figure 6a and b demonstrate that pH and concentration have a more significant effect on SPR intensity than time. Furthermore, concentration has the greatest impact on the synthesis of Ag nanoparticles (Fig. 6c). The normal probability plot in Fig. 7a indicates that all the residual values lie along a straight line with no big deviations and follow a normal distribution. The scatter plot in Fig. 7b demonstrates that the residuals are both random and within the ± 3σ limits.

Heavy metal removal (Fe and Zn) studies

Experiments were conducted to compare the effectiveness of bare and immobilized phyco-synthesized

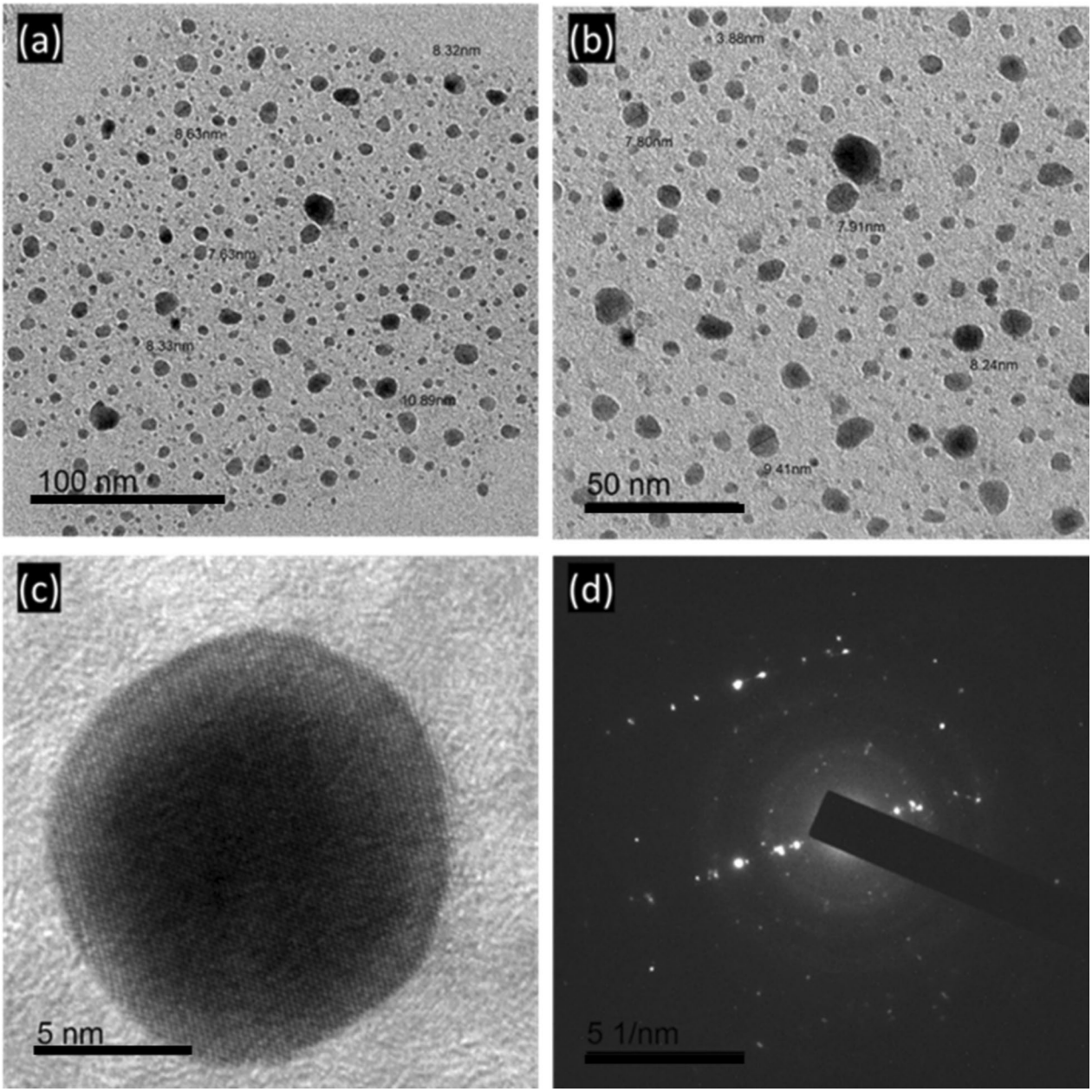


Fig. 3 TEM micrograph of phyco-synthesized Ag-FeBNPs in three magnifications **a**100 nm, **b** 50 nm, **c** 5 nm, and **d** SAED pattern

Ag-FeBNPs in Fe and Zn removal from fish aquaculture wastewater effluents (Fig. 8). Ag-FeBNPs@Alg beads are spherical of similar size with fairly homogeneous size distribution (3–4 mm), as shown in Fig. 8b. With bare Ag-FeBNPs, the Fe and Zn concentrations decreased from 18.5 mg/L and 5.7 mg/L to 1.0 mg/L (94.8% removal) and 1.4 mg/L (76.0% removal), respectively (Table 3). Using Ag-FeBNPs@Alg beads the % of removal of Fe is 78.0% and reached 45.5% for Zn (Fig. 9).

Characteristics of Ag-FeBNPs@Alg beads before and after heavy metal removal

The SEM micrograph of FeBNPs@Alg beads shows the particles of Ag-FeBNPs were in a delicately dispersed state within the alginate matrix with a porous surface (Fig. 10a). The surface of the Ag-FeBNPs@Alg bead after

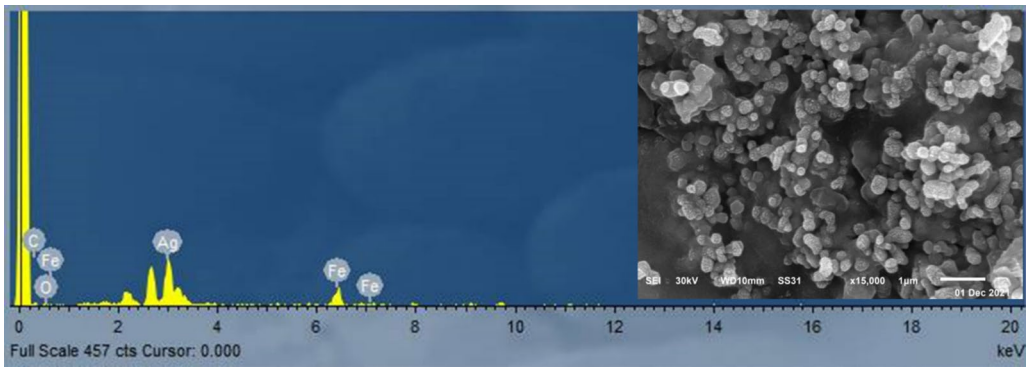


Fig. 4 EDAX spectra of phyco-synthesized Ag-FeBNPs. The inset figure is the SEM micrograph

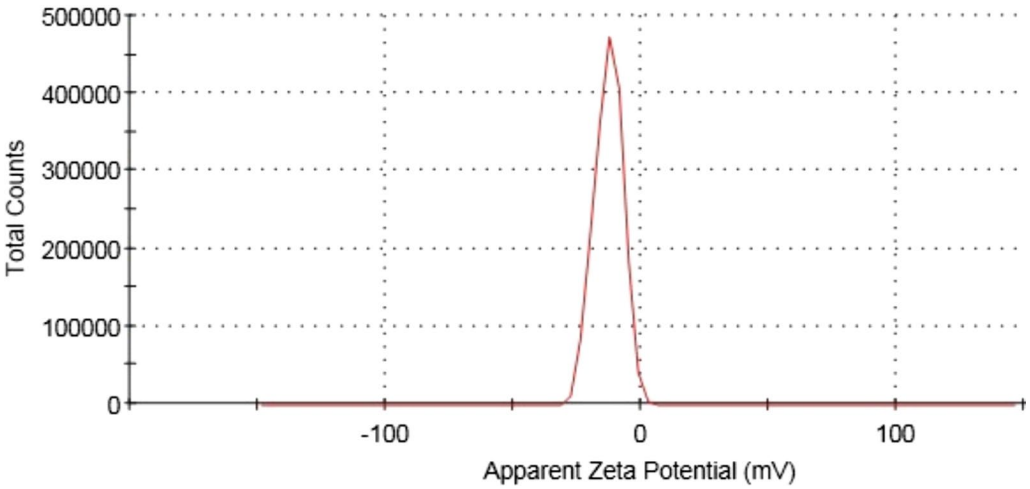


Fig. 5 Zeta potential of phyco-synthesized Ag-FeBNPs

heavy metal removal (Fig. 10b) is represented by peak and valley topography. It also appears to be quite heterogeneous and uneven.

FTIR spectrum of Ag-FeBNPs@Alg beads before heavy metal removal (Fig. 11a) shows number of characteristic absorption peaks at 3286 cm^{-1}, 2372 cm^{-1}, 2317 cm^{-1}, 1622 cm^{-1}, 1415 cm^{-1}, 1092 cm^{-1}, and 1030 cm^{-1}. FTIR spectrum of Ag-FeBNPs@Alg beads after heavy metal removal (Fig. 11b) shows the peak shift located at about 1632 and 2366 cm^{-1} while the peaks at 2317, 1415, and 1030 cm^{-1} became weaker and shifted. Also, the peak at 1092 cm^{-1} disappeared.

Evaluation of the reuse potentiality of Ag-FeBNPs@Alg beads

Adsorption–desorption experiments were carried out to evaluate the reuse potentiality of Ag-FeBNPs@Alg beads. As shown in Table 4, the % of Zn removal decreased from 86.5 to 57.2% whereas the % of Fe removal decreased from 38.7 to 16.9% after three runs and recorded no removal in the four runs. The results indicated that Ag-FeBNPs@Alg beads can be reused up to four times with negligible loss of removal efficiency of Zn and Fe. However, a decrease in efficiency was observed in the fourth run for Fe (Table 4).

Discussion

Nano-bioremediation is promising for revolutionizing water treatment as it can be used to remediate water contaminated with diverse pollutants, including heavy metals, organic contaminants, and pesticides [45]. Biologically produced NPs have emerged as an efficient alternative to traditional methods in nano-bioremediation due to their biocompatibility, environmental friendliness, and wide scalability [46]. This study focuses on the phyco-synthesis of Ag-FeBNPs from the extract of *Laurencia papillosa*. The observed color transition is primarily due to the algal-mediated reduction, stabilization, and capping of Ag and Fe ions [47] and to the surface plasmon response of the phyco-synthesized Ag-FeBNPs [48].

Table 2 Specifics of the 20 runs that were carried out utilizing CDD to improve the phyco-synthesis of Ag-FeBNPs *using Laurencia papillosa* extract

Runs	pH	The concentration of algal extract (g/100 mL)	Incubation time (min)	SPR_{263}
1	8.6	4.9	44	4.53
2	6.5	10.5	95	8.18
3	4.4	4.9	146	4.88
4	8.6	16.1	146	9.76
5	6.5	10.5	95	7.92
6	4.4	4.9	44	4.68
7	8.6	4.9	146	4.86
8	6.5	10.5	95	7.98
9	8.6	16.1	44	9.3
10	6.5	10.5	95	8.16
11	4.4	16.1	44	7.12
12	4.4	16.1	146	8.37
13	3	10.5	95	7.58
14	6.5	20	95	5.96
15	6.5	10.5	95	8.65
16	**10**	**10.5**	**95**	**11**
17	6.5	1	95	3.15
18	6.5	10.5	10	7.99
19	6.5	10.5	180	8.31
20	6.5	10.5	95	7.92

This indicates the mechanism of electron transfer from polyphenolic compounds in *L. Papillosa* to the metal ions, resulting in the reduction and nucleation of Ag and Fe nanoparticles.

The diffraction peaks observed in the XRD pattern of Ag-FeBNPs were consistent with the standard patterns of Ag (JCPDS no. 04-0783) and Fe (JCPDS no. 33-0664), supporting the formation of bimetallic phases [33]. The O–H stretching vibration observed at 3421 cm^{-1} in the FTIR spectrum of *L. papillosa* aqueous extracts confirmed the presence of polyphenolic and saccharide compounds [49]. The existence of a peak shift at 3421 cm^{-1}, indicates a major involvement of O–H of the phenol groups that are present in algal extracts [50]. The absorption peak that appeared at 1598 cm^{-1} likely indicates the presence of C=O bond stretching in aromatic compounds within the algal extract [51]. The characteristic peaks at 1384 cm^{-1}, 1035 cm^{-1}, 672 cm^{-1}, and 865 cm^{-1} indicated the presence of nitro groups, primary alcohols, aromatic rings, and vinyl groups, respectively [52]. The minor shifts and slight changes observed in the FTIR spectra of AgFeBNPs suggested that biomolecules from the extracts were capped onto the AgFeBNPs [53]. This capping mechanism provides stability and prevents nanoparticle agglomeration by surface chemical interactions with hydroxyl, carbonyl, and nitro groups. These findings align with prior studies [54, 55]. The TEM images of Ag-FeBNPs displayed a nano range spherical shaped morphology with no aggregation or agglomeration with particles that ranged from 10.17 to 19.99 nm. These observations are consistent with previous observations [33]. The characteristic ring patterns observed in the SAED pattern indicated the polycrystalline structure of Ag-FeBNPs [56]. The Ag and Fe peaks were observed in the EDAX spectrum, indicating the successful formation of Ag-FeBNPs [33]. The additional peaks likely resulted from algal biomolecule interactions during the synthesis process [57]. The SEM micrograph showed that some nanoparticles agglomerated together to form larger irregular clusters with uniform surfaces, such highly conglomerated NPs are evidence of agglomeration; in agreement with prior literature [58]. The Ag-FeBNPs show negative potential values of 17.2 mV [59]. Biomolecules in the algal extract may inhibit the positive potential of the NPs [60].

CCD proved to be a valuable tool for optimizing the phyco-synthesis of Ag-FeBNPs from *L. papillosa* extract by modeling the complex interactions among experimental variables [61]. Multivariate optimization was performed using 3D response surface analysis to determine the optimal value of each parameter for maximum production of Ag-FeBNPs [62, 63]. Application of this model helps us to indicate that pH and concentration of algal extract were the most significant factors, while time was an insignificant parameter. The normal probability plot indicated a good fit between the residuals and a normal distribution [64]. The proposed linear model exhibits no significant bias or systematic error, demonstrating its suitability for the optimization of the phycho-synthesis process of Ag-FeBNPs [65].

The performance of bare Ag-FeBNPs in removing heavy metals (Fe and Zn) surpassed that of previous studies documented by Karatapanis et al. and Yadav et al. [66, 67]. Comparative analysis shows that the removal efficiency of Fe (94.8%) and Zn (76.0%) in this study is higher than that reported for monometallic AgNPs or FeNPs, indicating the benefits of bimetallic composition [68, 69]. The high heavy metal removal using Ag-FeBNPs, when compared with AgNPs and FeNPs, could be attributed to the high surface area, the availability of high adsorption sites, and their enhanced properties as compared to their monometallic, which can improve the heavy metal removal [70–72]. This study also tested the use of alginate beads as a good trial to eliminate the potential toxicity of using bare NPs, which was reported in many reports [73, 74]. Reduced mobility of Ag-FeBNPs can be achieved through immobilization in Ca-alginate polymer as it is a non-toxic, biodegradable, and water-insoluble polymer

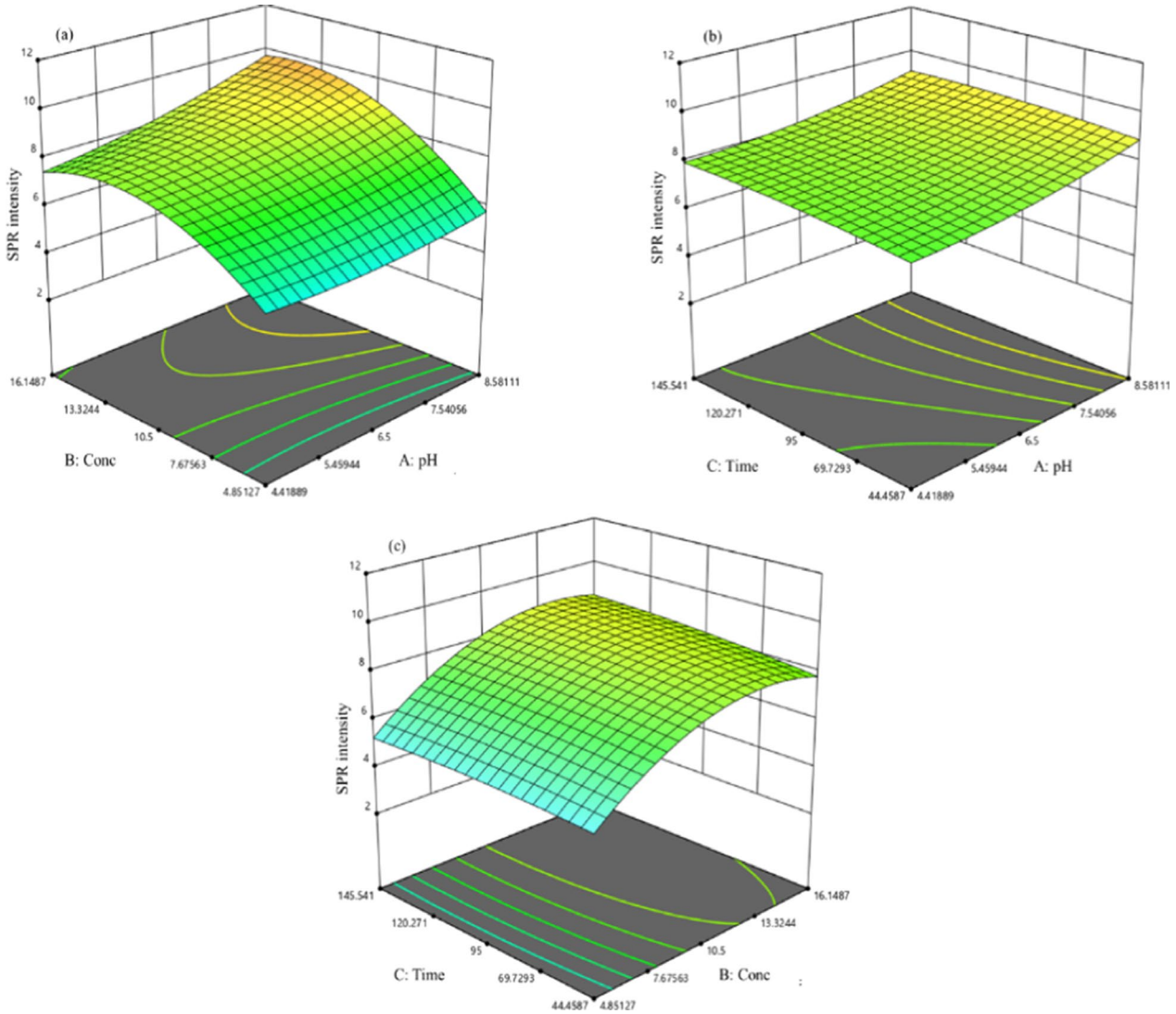


Fig. 6 The 3D response surface plots of independent parameters; **a** concentration-pH, **b** pH-time, and **c** time-concentration, influencing the SPR intensity of Ag-FeBNPs phyco-synthesis using *Laurencia papillosa* extract

[75]. Ag-FeBNPs@Alg beads exhibited slightly lower Fe and Zn removal efficiency compared to bare Ag-FeBNPs. This may be due to the alginate matrix surrounding Ag-FeBNPs may have hindered the diffusion of Fe and Zn ions to the NPs surface [76]. Ag-FeBNPs remove pollutants mainly through surface adsorption, complexation, and redox reactions. Fe facilitates electron transfer and the reduction of toxic metals, while Ag enhances stability and catalytic activity, resulting in a bimetallic system with superior efficiency compared to monometallic NPs [2]. Ag-FeBNPs@Alg beads adsorption mechanism. Embedding Ag-FeBNPs in alginate beads improves performance by providing extra carboxyl and hydroxyl groups for adsorption and ion exchange, preventing nanoparticle aggregation, and enabling easy recovery and reuse [77, 78]. The porous alginate matrix facilitates mass transfer of heavy metal ions to the nanoparticle surface, maintaining redox and catalytic activity while minimizing leaching, which explains the slightly lower removal efficiency compared to bare NPs [42].

The surface morphology of Ag-FeBNPs@Alg beads before heavy metal showed that NPs were very uniformly distributed on the beads' surface and the surfaces of the beads also showed obvious porous structures, similar to other previously reported results [79]. However, after heavy metal removal, the beads appeared in more irregular shapes with rougher surfaces with voids and rifts. These observed morphology changes can be

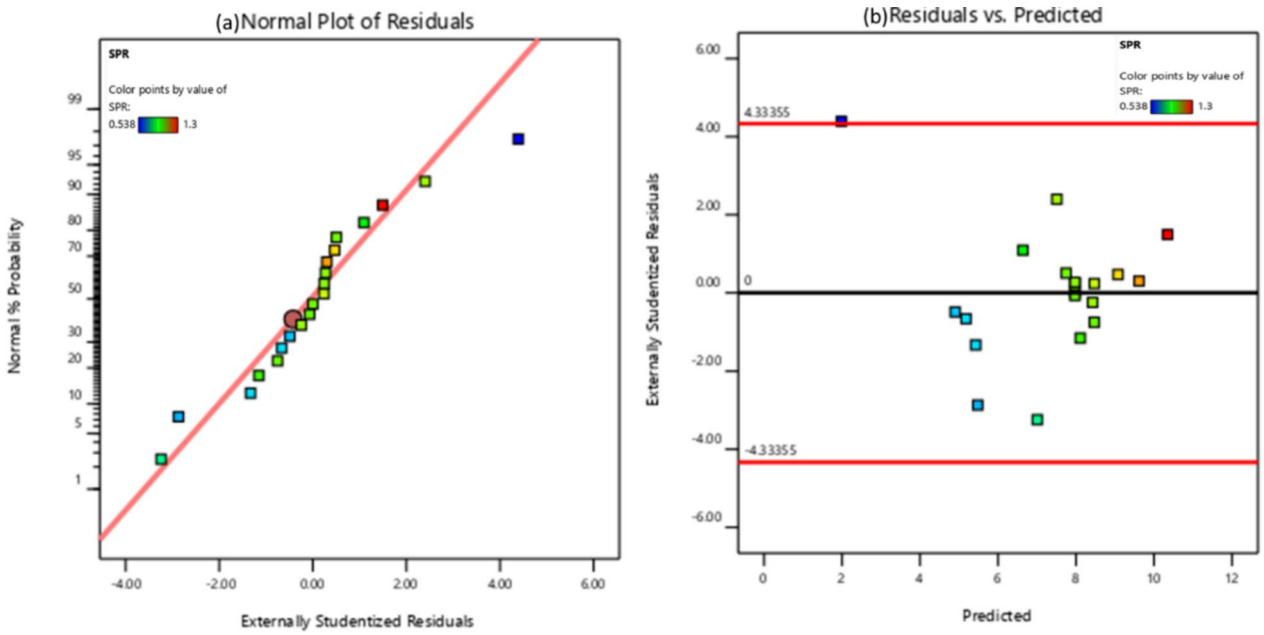


Fig. 7 **a** The normal probability plot and **b** The scatter plot of residuals versus predicted SPR intensity of the phyco-synthesized Ag-FeBNPs *using Laurencia papillosa* extract

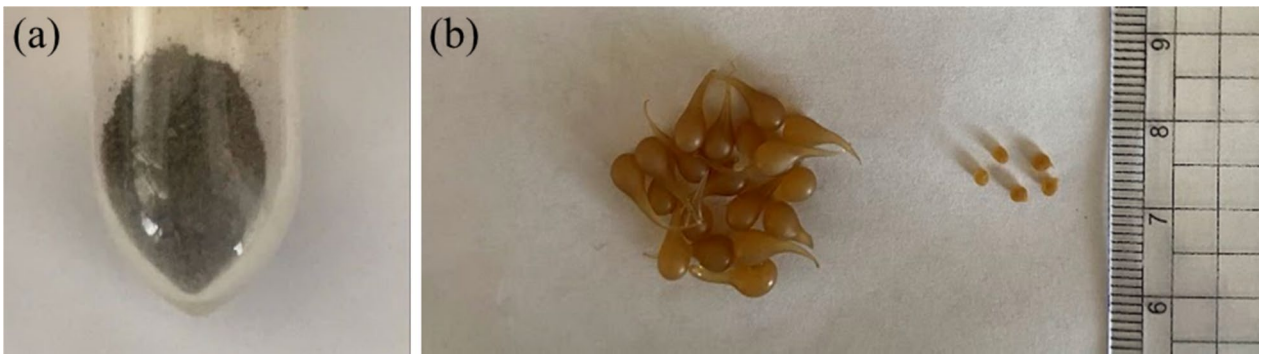


Fig. 8 Images of **a** bare Ag-FeBNPs and **b** Ag-FeBNPs@Alg beads; the hydrated beads are on the left and the dry beads are on the right

Table 3 Fe and Zn concentrations from aquaculture wastewater effluent before and after treatment with bare Ag-FeBNPs and Ag-FeBNPs@Alg beads

NPs type	Elements	Conc before treatment (mg/L)	Conc after treatment (mg/L)	% Of heavy metal removal
Bare Ag-FeBNPs	Fe	18.5	1.0	94.8
	Zn	5.7	1.4	76.0
Ag-FeBNPs@Alg beads	Fe	18.5	4.1	78.0
	Zn	5.7	3.1	45.5

attributed to the formation of metal-carboxyl and metal-hydroxyl complexes, which modify the bead surface and create rifts and voids observed in SEM [80]. Characteristic peaks at 3310 cm^{-1} and 1030 cm^{-1} in the FTIR spectrum before heavy metal removal indicated the presence of –OH and C–O stretching vibrations, suggesting the existence of hydroxyl groups. The obtained results were in good agreement with the previous studies [81].

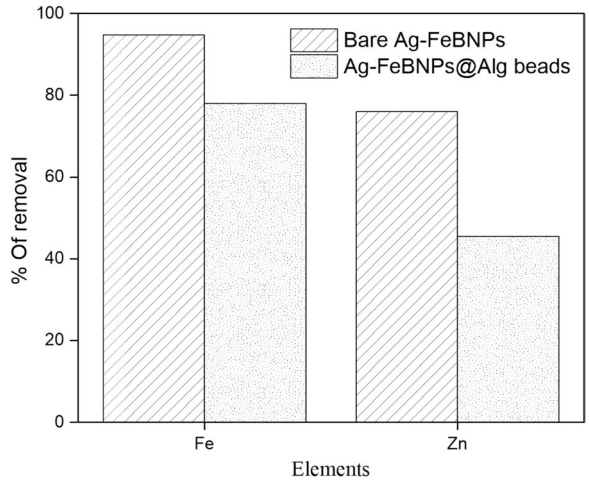


Fig. 9 Comparison of heavy metal (Fe and Zn) removal efficiency of bare Ag-FeBNPs and Ag-FeBNPs@Alg beads from aquaculture wastewater effluent

The bands around 1625 cm^{-1} and 1411 cm^{-1} are indicative of C=O stretching vibrations in the carboxyl groups [82]. The FTIR spectra of the beads after heavy metal removal showed a significant shift in these bands [83]. The absence of significant changes in infrared spectra implies the adsorption process is physically mechanism-oriented [84].

The reuse potentiality of Ag-FeBNPs@Alg beads has been investigated as it is likely to be a key factor in accessing the potential of the beads for commercial applications [85]. Even after four runs of reuse of Ag-FeBNPs@Alg beads, the percentage of Zn removal decreased from 86.5 to 57.2%, and the percentage of Fe removal decreased from 38.7 to 16.9%. Hence, the immobilization of Ag-FeBNPs in alg beads facilitated easy filtration and was successfully applied for heavy metals (Zn, and Fe) removal from fish aquaculture wastewater effluents. Ag-FeBNPs@Alg beads are thus well-suited for use in both large- and small-scale treatment facilities, as well as infield operations. To assess the cost-effectiveness of this process, the main raw materials were considered. The silver precursor ($AgNO_3$) represents the primary cost driver, with typical catalogue prices of ≈ 3–4 USD/g, while iron salts ($FeCl_3$ or $FeSO_4$) are comparatively inexpensive (< 1 USD/100 g in bulk). Sodium alginate, required for immobilization, is widely available at ≈ 5–20 USD/kg, and the crosslinker $CaCl_2$ is very low-cost (tens of USD per kg). *Laurencia papillosa* biomass is locally available in coastal regions and can be obtained at minimal cost compared to synthetic reagents. Importantly, immobilization of Ag-FeBNPs in alginate beads not only improves dispersibility but also allows reuse even after four runs of reuse, thereby lowering the effective treatment cost per cycle and supporting scalability for aquaculture wastewater remediation. The findings of this study demonstrate the potential of Ag-FeBNPs@Alg beads as a practical and sustainable tool for wastewater treatment, particularly in aquaculture systems where heavy metal accumulation threatens water quality and aquatic health. The enhanced dispersibility of Ag-FeBNPs within the alginate matrix significantly improves their efficiency in nano-bioremediation of various wastewater contaminants. Their high adsorption efficiency, stability, and reusability highlight their suitability for large-scale applications in environmental remediation and green nanotechnology-based water purification systems. Moreover, these beads can be repurposed as a nutrient-rich fertilizer, as the adsorbed nutrients may serve as valuable components for agricultural applications[86].

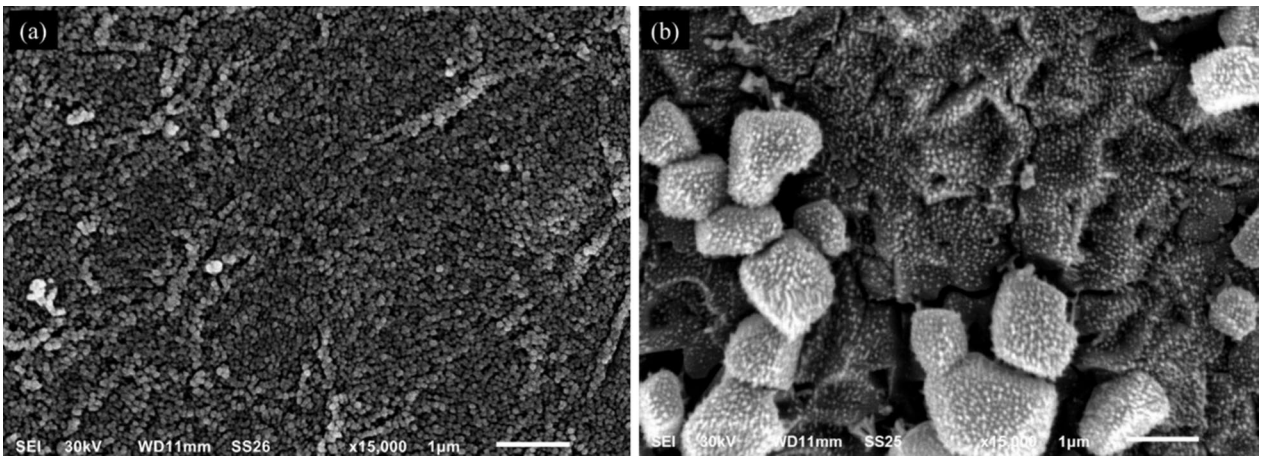


Fig. 10 SEM micrograph of Ag-FeBNPs@Alg beads **a** before and **b** after heavy metal removal

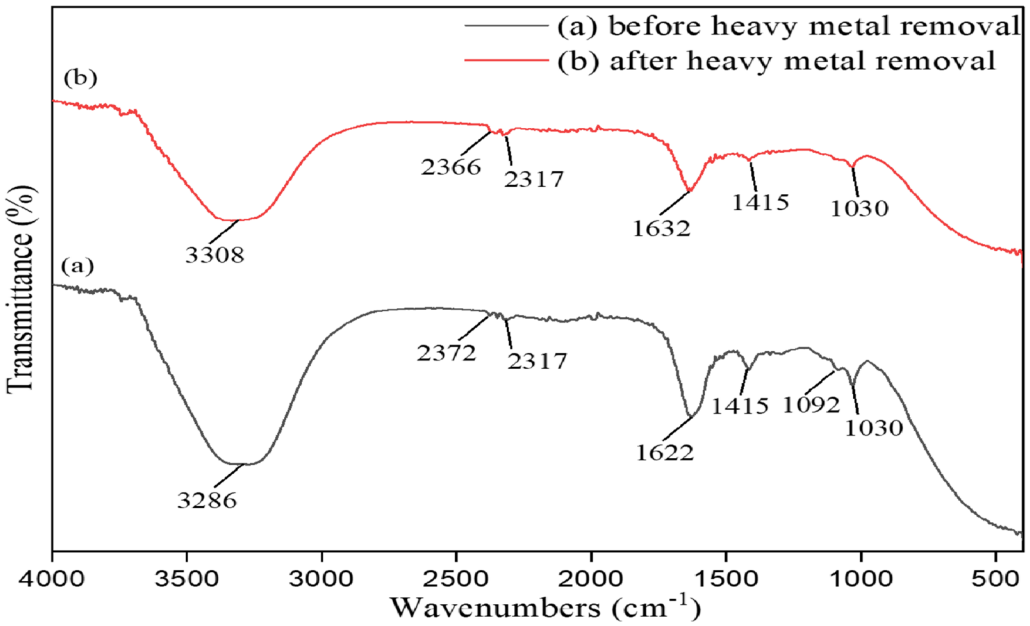


Fig. 11 FTIR spectrum of Ag-FeBNPs@Alg beads **a** before and **b** after heavy metal removal

Conclusion

This study demonstrated for the first time the feasibility of using *Laurencia papillosa* for phyco-synthesis of Ag-FeBNPs providing a sustainable and environmentally friendly approach to the green synthesis of nanoparticles. The process of phyco-synthesis was improved by using central composite design (CCD), avoiding potential errors and time-consuming of the classical methods. Also, immobilization of Ag-FeBNPs in alginate beads and comparison of the reactivity of bare Ag-FeBNPs and Ag-FeBNPs@Alg beads toward heavy removal from fish aquaculture wastewater effluents. The % of Fe removal using bare Ag-FeBNPs and Ag-FeBNPs@Alg beads were 94.8% and 78.0%, respectively whereas the % of Zn removal was 76.0% and 45.5% respectively. The simplicity of Ag-FeBNPs@Alg beads preparation, biodegradability, practical utility, and relatively low preparation cost reveal their utility as an adsorbent for heavy metal removal. Extensive investigations of Ag-FeBNPs@Alg beads at a commercial scale may uncover new opportunities for their application in heavy metal remediation. Nevertheless, the present study is constrained by limited replicates and the absence of detailed adsorption modeling, which will be addressed in future investigations to provide stronger statistical validation and deeper mechanistic insights. Overall, this study is significant as it evaluates, for the first time, the performance of both bare and immobilized Ag-FeBNPs in removing Fe and Zn from aquaculture wastewater. The comparison highlights the novelty of alginate immobilization, which not only enhances stability and adsorption efficiency but also facilitates recovery and reuse. These findings provide a practical and eco-friendly approach for advancing bioremediation applications in contaminated water systems.

Table 4 Percentage of heavy metal (Zn and Fe) removal from wastewater effluent of aquaculture after treatment with Ag-FeBNPs@Alg for four reuse runs

Elements	Reuse runs (% of heavy metal removal)			
	First	Second	Third	Fourth
Zn	86.5	82.5	82.1	57.2
Fe	38.7	34.1	16.9	0.0

Acknowledgements
The authors would like to express their sincere gratitude to the National Authority for Remote Sensing & Space Sciences (NARSS)- Egypt for their invaluable support and contributions to this research.

Author contribution
Elham M. Ali, Ahlam S. El Shehawy, and Ashraf Elsayed were responsible for the presented idea. Ahlam S. El Shehawy carried out the experiments. Ahlam S. El Shehawy wrote the manuscript with support from Elham M. Ali and Ashraf Elsayed. Elham M. Ali and Ashraf Elsayed were involved in planning and supervised the work.

Funding
Open access funding provided by The Science, Technology & Innovation Funding Authority (STDF) in cooperation with The Egyptian Knowledge Bank (EKB). The financial support for this research was provided by the Science, Technology & Innovation Funding Authority (STDF), Egypt through a Post Graduate Support Grant (PGSG), Non-Industrial sector, National, grant number 45049.

Availability of data and materials
The datasets used and/or analyzed during this study are available from the corresponding author on reasonable request.

Declarations

Ethics approval and consent to participate
Not applicable.

Consent for publication
Not applicable.

Competing interests
The authors declare no competing interests.

Author details
[1]Department of Botany, Faculty of Sciences, University of Mansoura, Mansoura, Egypt. [2]Department of Aquatic Environment, Faculty of Fish Resources, University of Suez, Suez, Egypt. [3]Department of Environmental Studies, The National Authority for Remote Sensing and Space Sciences (NARSS), Cairo, Egypt.

Received: 6 April 2025 Accepted: 29 November 2025
Published online: 15 January 2026

References

1. Sonone SS, Jadhav S, Sankhla MS, Kumar R (2020) Water contamination by heavy metals and their toxic effect on aquaculture and human health through food chain. Lett Appl NanoBiosci 10(2):2148–2166
2. Samuel MS, Selvarajan E, Sarswat A, Muthukumar H, Jacob JM, Mukesh M et al (2022) Nanomaterials as adsorbents for As (III) and As (V) removal from water: a review. J Hazard Mater 424:127572
3. Emmanuel UC, Chukwudi MI, Monday SS, Anthony AI (2022) Human health risk assessment of heavy metals in drinking water sources in three senatorial districts of Anambra State, Nigeria. Toxicol Rep 9:869–875
4. Samuel MS, Ravikumar M, Raizada P, Azelee NIW, Selvarajan E, Selvasembian R (2023) Recent progress on the remediation of dyes in wastewater using cellulose-based adsorbents. Ind Crops Prod 206:117590
5. Samuel MS, Shang M, Klimchuk S, Niu J (2021) Novel regenerative hybrid composite adsorbent with improved removal capacity for lead ions in water. Ind Eng Chem Res 60(14):5124–5132
6. Vishnu D, Rajendran A, Dhandapani B (2024) A potent insight into the microalgal and surface-modified magnetic microalgal biomass synthesis and treatment strategies in the removal of selenium and chromium metal ions. Energy Ecol Environ 9(2):113–129
7. Kumar R, Kundu D, Kormoker T, Joshi S, Rose PK, Kumar S et al (2024) Phycoremediation of potentially toxic elements for agricultural and industrial wastewater treatment: recent advances, challenges, and future prospects. Desalin Water Treat 319:100505
8. Guo D, Xie G, Luo J (2013) Mechanical properties of nanoparticles: basics and applications. J Phys D Appl Phys 47(1):013001
9. Ali EM, El-Shehawy AS (2023) Metallic nanoparticles and bioremediation for wastewater treatment. Advanced application of nanotechnology to industrial wastewater. Springer, pp 215–239
10. Samuel MS, Selvarajan E, Chidambaram R, Patel H, Brindhadevi K (2021) Clean approach for chromium removal in aqueous environments and role of nanomaterials in bioremediation: present research and future perspective. Chemosphere 284:131368
11. Unnisa A, Greig NH, Kamal MA (2023) Nanotechnology: a promising targeted drug delivery system for brain tumours and Alzheimer's disease. Curr Med Chem 30(3):255–270
12. Zou Y, Wang X, Khan A, Wang P, Liu Y, Alsaedi A et al (2016) Environmental remediation and application of nanoscale zero-valent iron and its composites for the removal of heavy metal ions: a review. Environ Sci Technol 50(14):7290–7304
13. Sivalingam AM, Pandian A (2024) Identification and characterization of silver nanoparticles from *Erythrina indica* and its antioxidant and Uropathogenic antimicrobial properties. Microb Pathog 190:106635
14. Junior AR, Yokaichiya F, Monerjan E, Lemke K, Guilger-Casagrande M, Lima R et al (2024) Structural characterization of silver nanoparticles produced by biogenic synthesis using SAXS. Phys B Condens Matter 684:415969
15. Karthik L, Kirthi AV, Ranjan S, Srinivasan VM (2019) Biological synthesis of nanoparticles and their applications. CRC Press
16. Samuel MS, Datta S, Chandrasekar N, Balaji R, Selvarajan E, Vuppala S (2021) Biogenic synthesis of iron oxide nanoparticles using *Enterococcus faecalis*: adsorption of hexavalent chromium from aqueous solution and in vitro cytotoxicity analysis. Nanomaterials 11(12):3290
17. El Shehawy AS, Elsayed A, El-Shehaby OA, Ali EM (2023) Algae-mediated synthesis and structural characterization of silver nanoparticles from *Laurencia papillosa* and *Galaxaura rugosa*. Egypt J Aquat Biol Fish 27(2):645–659
18. Vinayagam R, Nagendran V, Goveas LC, Narasimhan MK, Varadavenkatesan T, Chandrasekar N et al (2024) Structural characterization of marine macroalgae derived silver nanoparticles and their colorimetric sensing of hydrogen peroxide. Mater Chem Phys 313:128787
19. Bamal D, Singh A, Chaudhary G, Kumar M, Singh M, Rani N et al (2021) Silver nanoparticles biosynthesis, characterization, antimicrobial activities, applications, cytotoxicity and safety issues: an updated review. Nanomaterials 11(8):2086
20. Zahoor M, Nazir N, Iftikhar M, Naz S, Zekker I, Burlakovs J et al (2021) A review on silver nanoparticles: classification, various methods of synthesis, and their potential roles in biomedical applications and water treatment. Water 13(16):2216
21. Lawrence LV, Vishnu D (2025) Exploring the potential of biologically synthesized nano-adsorbents in removal of hexavalent chromium (Cr (VI)): mechanistic studies and circular economy integration. J Environ Manage 388:126012
22. Heisnam P, Moirangthem A, Singh YD, Dutta P, Devi CV, Hazarika B (2022) Exploitation of silver nanoparticles in bioremediation. CRC Press, Bioremediation, pp 143–155
23. Chaudhari DS, Upadhyay RP, Shinde GY, Gawande MB, Filip J, Varma RS et al (2024) A review on sustainable iron oxide nanoparticles: syntheses and applications in organic catalysis and environmental remediation. Green Chem 26(13):7579–7655
24. Yazdanparast S, Benvidi A, Azimzadeh M, Tezerjani MD, Ghaani MR (2020) Experimental and theoretical study for miR-155 detection through resveratrol interaction with nucleic acids using magnetic core-shell nanoparticles. Microchim Acta 187(8):1–10
25. Al-Enazi NM (2022) Optimized synthesis of mono and bimetallic nanoparticles mediated by unicellular algal (diatom) and its efficiency to degrade azo dyes for wastewater treatment. Chemosphere. https://doi.org/10.1016/j.chemosphere.2022.135068
26. Padilla-Cruz AL, Garza-Cervantes JA, Vasto-Anzaldo XG, García-Rivas G, León-Buitimea A, Morones-Ramírez JR (2021) Synthesis and design of Ag–Fe bimetallic nanoparticles as antimicrobial synergistic combination therapies against clinically relevant pathogens. Sci Rep 11(1):5351
27. Bundschuh M, Filser J, Lüderwald S, McKee MS, Metreveli G, Schaumann GE et al (2018) Nanoparticles in the environment: where do we come from, where do we go to? Environ Sci Eur 30(1):1–17
28. Matricardi P, Pontoriero M, Coviello T, Casadei MA, Alhaique F (2008) In situ cross-linkable novel alginate-dextran methacrylate IPN hydrogels for biomedical applications: mechanical characterization and drug delivery properties. Biomacromol 9(7):2014–2020
29. Aziz F, El Achaby M, Lissaneddine A, Aziz K, Ouazzani N, Mamouni R et al (2020) Composites with alginate beads: a novel design of nano-adsorbents impregnation for large-scale continuous flow wastewater treatment pilots. Saudi J Biol Sci 27(10):2499–2508
30. John JA, Samuel MS, Selvarajan E (2023) Immobilized cellulase on Fe3O4/GO/CS nanocomposite as a magnetically recyclable catalyst for biofuel application. Fuel 333:126364
31. Somasundaram CK, Atchudan R, Edison TNJI, Perumal S, Vinodh R, Sundramoorthy AK et al (2021) Sustainable synthesis of silver nanoparticles using marine algae for catalytic degradation of methylene blue. Catalysts 11(11):1377
32. Kumar P, Senthamil Selvi S, Govindaraju M (2013) Seaweed-mediated biosynthesis of silver nanoparticles using *Gracilaria corticata* for its antifungal activity against *Candida* spp. Appl Nanosci 3:495–500

33. Malik MA, Alshehri AA, Patel R (2021) Facile one-pot green synthesis of Ag–Fe bimetallic nanoparticles and their catalytic capability for 4-nitrophenol reduction. J Mater Res Technol 12:455–470
34. Nyakundi EO, Padmanabhan MN (2015) Green chemistry focus on optimization of silver nanoparticles using response surface methodology (RSM) and mosquitocidal activity: *Anopheles stephensi* (Diptera: Culicidae). Spectrochim Acta A Mol Biomol Spectrosc 149:978–984
35. Rose PK, Kumar R, Kumar R, Kumar M, Sharma P (2023) Congo red dye adsorption onto cationic amino-modified walnut shell: characterization, RSM optimization, isotherms, kinetics, and mechanism studies. Groundw Sustain Dev 21:100931
36. Bezbaruah AN, Krajangpan S, Chisholm BJ, Khan E, Bermudez JJE (2009) Entrapment of iron nanoparticles in calcium alginate beads for groundwater remediation applications. J Hazard Mater 166(2–3):1339–1343
37. Sharma R, Bisen D, Shukla U, Sharma B (2012) X-ray diffraction: a powerful method of characterizing nanomaterials. Recent Res Sci Technol 4(8):77–79
38. Wen S, Richardson T, Ghantous D, Striebel K, Ross hP, Cairns E (1996) FTIR characterization of PEO+ LiN (CF3SO2) 2 electrolytes. J Electroanal Chem 408(1–2):113–118
39. Fultz B, Howe JM (2012) Transmission electron microscopy and diffractometry of materials. Springer Science & Business Media
40. Pradhan S (2013) Comparative analysis of silver nanoparticles prepared from different plant extracts (*Hibiscus rosa sinensis, Moringa oleifera, Acorus calamus, Cucurbita maxima, Azadirachta indica*) through green synthesis method
41. Hanaor D, Michelazzi M, Leonelli C, Sorrell CC (2012) The effects of carboxylic acids on the aqueous dispersion and electrophoretic deposition of ZrO2. J Eur Ceram Soc 32(1):235–244
42. Tiwari A, Soni A, Bajpai A (2012) Nanoparticles loaded alginate beads as potential adsorbent for removal of phenol from aqueous solution. Synth React Inorg, Met-Org, Nano-Met Chem 42(8):1158–1166
43. Aleem A (1993) The marine algae of Alexandria. Egypt Alexandria 55
44. Lima A, Gaspar R, Neto J, Pereira L (2017) The identification of macroalgae and the assessment of intertidal rocky shores' ecological statuses in the central western coast of continental Portugal. Chapter 2. Seaweeds biodiversity, environmental chemistry and ecological impacts Hauppauge. Nova Science Publishers Inc, NewYork, pp 19–84
45. Hidangmayum A, Debnath A, Guru A, Singh B, Upadhyay S, Dwivedi P (2022) Mechanistic and recent updates in nano-bioremediation for developing green technology to alleviate agricultural contaminants. Int J Environ Sci Technol, pp 1–26
46. Fareed N, Nisa S, Bibi Y, Fareed A, Ahmed W, Sabir M et al (2023) Green synthesized silver nanoparticles using carrot extract exhibited strong antibacterial activity against multidrug resistant bacteria. J King Saud Univ Sci 35(2):102477
47. Thiurunavukkarau R, Shanmugam S, Subramanian K, Pandi P, Muralitharan G, Arokiarajan M et al (2022) Silver nanoparticles synthesized from the seaweed *Sargassum polycystum* and screening for their biological potential. Sci Rep 12(1):1–11
48. Shantkriti S, Pradeep M, Unish K, Das V, Nidhin S, Gugan K et al (2023) Bioynthesis of silver nanoparticles using *Dunaliella salina* and its antibacterial applications. Appl Surf Sci Adv 13:100377
49. Balaraman P, Balasubramanian B, Kaliannan D, Durai M, Kamyab H, Park S et al (2020) Phyco-synthesis of silver nanoparticles mediated from marine algae *Sargassum myriocystum* and its potential biological and environmental applications. Waste Biomass Valoriz 11:5255–5271
50. Rasheed T, Bilal M, Li C, Nabeel F, Khalid M, Iqbal HM (2018) Catalytic potential of bio-synthesized silver nanoparticles using *Convolvulus arvensis* extract for the degradation of environmental pollutants. J Photochem Photobiol B Biol 181:44–52
51. Venkateswarlu S, Kumar BN, Prathima B, SubbaRao Y, Jyothi NVV (2019) A novel green synthesis of Fe3O4 magnetic nanorods using *Punica granatum* rind extract and its application for removal of Pb (II) from aqueous environment. Arab J Chem 12(4):588–596
52. Vardin H, Tay A, Ozen B, Mauer L (2008) Authentication of pomegranate juice concentrate using FTIR spectroscopy and chemometrics. Food Chem 108(2):742–748
53. El-Kassas HY, El Komi MM (2014) Biogenic silver nanoparticles using seaweed *Ulva rigida* and their fungicidal and cytotoxic effects. J King Abdulaziz Univ Mar Sci 25:3–20
54. Algotiml R, Gab-Alla A, Seoudi R, Abulreesh HH, El-Readi MZ, Elbanna K (2022) Anticancer and antimicrobial activity of biosynthesized Red Sea marine algal silver nanoparticles. Sci Rep 12(1):1–18
55. Carroll KJ, Hudgins DM, Spurgeon S, Kemner KM, Mishra B, Boyanov MI et al (2010) One-pot aqueous synthesis of Fe and Ag core/shell nanoparticles. Chem Mater 22(23):6291–6296
56. Łukowiec D, Radoń A (2020) Self-organization of silver nanoparticles during synthesis of Ag–Au nanoalloy by UV irradiation method. J Mater Sci 55(7):2796–2801
57. Abdel-Raouf N, Alharbi RM, Al-Enazi NM, Alkhulaifi MM, Ibraheem IBM (2018) Rapid biosynthesis of silver nanoparticles using the marine red alga *Laurencia catarinensis* and their characterization. Beni-Suef Univ J Basic Appl Sci 7(1):150–157
58. Kamli MR, Srivastava V, Hajrah NH, Sabir JS, Ali A, Malik MA et al (2021) Phytogenic fabrication of Ag–Fe bimetallic nanoparticles for cell cycle arrest and apoptosis signaling pathways in *Candida auris* by generating oxidative stress. Antioxidants 10(2):182
59. Mahmoodi NM, Keshavarzi S, Oveisi M, Rahimi S, Hayati B (2019) Metal-organic framework (ZIF-8)/inorganic nanofiber (Fe2O3) nanocomposite: green synthesis and photocatalytic degradation using LED irradiation. J Mol Liq 291:111333
60. Shi S-F, Jia J-F, Guo X-K, Zhao Y-P, Chen D-S, Guo Y-Y et al (2012) Biocompatibility of chitosan-coated iron oxide nanoparticles with osteoblast cells. Int J Nanomedicine. https://doi.org/10.2147/IJN.S34348
61. Saad WF, Othman AM, Abdel-Fattah M, Ahmad MS (2021) Response surface methodology as an approach for optimization of α-amylase production by the new isolated thermotolerant *Bacillus licheniformis* WF67 strain in submerged fermentation. Biocatal Agric Biotechnol 32:101944
62. Chowdhury S, Yusof F, Faruck MO, Sulaiman N (2016) Process optimization of silver nanoparticle synthesis using response surface methodology. Procedia Eng 148:992–999
63. Rose PK, Poonia V, Kumar R, Kataria N, Sharma P, Lamba J et al (2023) Congo red dye removal using modified banana leaves: adsorption equilibrium, kinetics, and reusability analysis. Groundw Sustain Dev 23:101005
64. Maghsoudy N, Azar PA, Tehrani MS, Husain SW, Larijani K (2019) Biosynthesis of Ag and Fe nanoparticles using *Erodium cicutarium*; study, optimization, and modeling of the antibacterial properties using response surface methodology. J Nanostruct Chem 9:203–216
65. Ibrahim S, Ahmad Z, Manzoor MZ, Mujahid M, Faheem Z, Adnan A (2021) Optimization for biogenic microbial synthesis of silver nanoparticles through response surface methodology, characterization, their antimicrobial, antioxidant, and catalytic potential. Sci Rep 11(1):770
66. Yadav VK, Amari A, Gacem A, Elboughdiri N, Eltayeb LB, Fulekar M (2023) Treatment of fly-ash-contaminated wastewater loaded with heavy metals by using fly-ash-synthesized iron oxide nanoparticles. Water 15(5):908
67. Karatapanis AE, Fiamegos Y, Stalikas CD (2011) Silica-modified magnetic nanoparticles functionalized with cetylpyridinium bromide for the preconcentration of metals after complexation with 8-hydroxyquinoline. Talanta 84(3):834–839
68. Ali A, Mannan A, Hussain I, Hussain I, Zia M (2018) Effective removal of metal ions from aquous solution by silver and zinc nanoparticles functionalized cellulose: isotherm, kinetics and statistical supposition of process. Environ Nanotechnol Monit Manag 9:1–11
69. Moraes LC, Gomes MP, Ribeiro-Andrade R, Garcia QS, Figueredo CC (2023) Green synthesized silver nanoparticles for iron and manganese ion removal from aqueous solutions. Environ Pollut 327:121483
70. Huang J, Fang F, Wang L, Shim J-J (2015) Removal of cobalt ions from aqueous solution by Ag/Fe bimetallic nanoparticles. Desalin Water Treat 56(8):2127–2134
71. Scaria J, Nidheesh P, Kumar MS (2020) Synthesis and applications of various bimetallic nanomaterials in water and wastewater treatment. J Environ Manage 259:110011
72. El Shehawy AS, Elsayed A, El-Shehaby OA, Ali EM (2023) Potentiality of the green synthesized silver nanoparticles for heavy metal removal using *Laurencia papillosa* seaweed. Egypt J Aquat Res. https://doi.org/10.1016/j.ejar.2023.10.001
73. Abbasi R, Shineh G, Mobaraki M, Doughty S, Tayebi L (2023) Structural parameters of nanoparticles affecting their toxicity for biomedical applications: a review. J Nanopart Res 25(3):43

74. Kumah EA, Fopa RD, Harati S, Boadu P, Zohoori FV, Pak T (2023) Human and environmental impacts of nanoparticles: a scoping review of the current literature. BMC Public Health 23(1):1–28
75. Mousa NE, Simonescu CM, Patescu RE, Lavric V, Culita DC (2017) Regeneration of calcium alginate and chitosan coated calcium alginate sorbents to be reused for lead (ii) removal from aqueous solutions. Rev Chim 68:1992–1996
76. Krajangpan S, Bermudez JJE, Bezbaruah AN, Chisholm BJ, Khan E (2008) Nitrate removal by entrapped zero-valent iron nanoparticles in calcium alginate. Water Sci Technol 58(11):2215–2222
77. Samuel MS, Shah SS, Bhattacharya J, Subramaniam K, Singh NP (2018) Adsorption of Pb (II) from aqueous solution using a magnetic chitosan/graphene oxide composite and its toxicity studies. Int J Biol Macromol 115:1142–1150
78. Samuel MS, Bhattacharya J, Raj S, Santhanam N, Singh H, Singh NP (2019) Efficient removal of Chromium (VI) from aqueous solution using chitosan grafted graphene oxide (CS-GO) nanocomposite. Int J Biol Macromol 121:285–292
79. Tzu TW, Tsuritani T, Sato K (2013) Sorption of Pb (II), Cd (II), and Ni (II) toxic metal ions by alginate-bentonite. J Environ Prot 4(1B):51
80. Pholnak P, Sittiyothee S, Sirisathitkul C, Sirisathitkul Y (2022) Dye removal efficiency of fresh and dry alginate beads incorporating zinc oxide. Arab J Basic Appl Sci 29(1):53–64
81. Elkholy R, Khalil E, Farag A, El-Fadl M, El-Aassar A (2020) Photocatalytic degradation of organic pollutants in wastewater using different nanomaterials immobilized on polymeric beads. Desalin Water Treat 193:117–128
82. Aziz F, El Achaby M, Lissaneddine A, Aziz K, Ouazzani N, Mamouni R, et al. (2019) Composites with alginate beads: a novel design of nano-adsorbents impregnation for large-scale continuous flow wastewater treatment pilots. Saudi J Biol Sci
83. Lin S, Huang R, Cheng Y, Liu J, Lau BL, Wiesner MR (2013) Silver nanoparticle-alginate composite beads for point-of-use drinking water disinfection. Water Res 47(12):3959–3965
84. Yin Z, Wang Y, Wang K, Zhang C (2018) The adsorption behavior of hydroxypropyl guar gum onto quartz sand. J Mol Liq 258:10–17
85. Almulaiky YQ, Al-Harbi SA (2022) Preparation of a calcium alginate-coated polypyrrole/silver nanocomposite for site-specific immobilization of polygalacturonase with high reusability and enhanced stability. Catal Lett 152:28–42
86. Wang B, Wan Y, Zheng Y, Lee X, Liu T, Yu Z et al (2019) Alginate-based composites for environmental applications: a critical review. Crit Rev Environ Sci Technol 49(4):318–356

Publisher's Note

Springer Nature remains neutral with regard to jurisdictional claims in published maps and institutional affiliations.